Electrical Impedance Tomography

Core Principles and Diagnostic EIT Development at Northwestern University

Sadi Eren Erenel

1. Introduction

Electrical Impedance Tomography (EIT) is a non-invasive, low-cost imaging modality that estimates internal electrical properties (specifically conductivity) by injecting small alternating currents through electrodes placed on the surface of an object and measuring the resulting voltage distribution. Biological tissues differ in conductivity due to composition, aeration, perfusion, and frequency-dependent electrical behavior, enabling EIT to visualize physiological processes in real time without ionizing radiation. Compared with conventional modalities such as CT or MRI, EIT offers advantages in portability, bedside monitoring capability, and minimal infrastructure requirements, making it particularly attractive in respiratory care and resource-limited settings (Teschner et al., 2010).

Although the first practical EIT systems emerged in the early 1980s, widespread clinical adoption has been gradual. Major barriers include the mathematically ill-posed nature of the inverse problem, sensitivity to measurement noise, and the need for high-quality hardware to ensure stable excitation and accurate voltage acquisition (Saulnier et al., 2001). Nevertheless, the past two decades have brought significant progress in both instrumentation and reconstruction methods. Advances in multiplexed excitation, low-noise differential measurement, and synchronous demodulation, particularly through the use of lock-in detection, have substantially improved signal fidelity (Brazey et al., 2022). Modern computational tools and finite-element solvers have further expanded the feasibility of robust three-dimensional imaging (Mansouri et al., 2021).

At the same time, open-source hardware initiatives have demonstrated that compact, replicable EIT systems can be built at low cost, lowering the entry barrier for laboratory research and accelerating translational development (Brazey et al., 2022; Creegan et al., 2024). As a result, clinical interest in EIT continues to grow.

Though still maturing, EIT's combination of real-time functional imaging, safety, affordability, and physiological sensitivity positions it as a promising supplement (or, in some contexts, an alternative) to conventional radiological techniques.

1.1 Tetrapolar (Four-Terminal) Measurement Method

Before examining the electrical hardware used in EIT systems, it is essential to understand how measurements are obtained. Modern EIT systems universally employ four-terminal (tetrapolar) measurements, in which two electrodes inject current and two separate electrodes measure the resulting voltage. This configuration is used because biological tissue and the electrode–skin interface introduce large and highly variable contact impedances. In a two-terminal measurement, the voltage drop across the electrode interface dominates the measurement, masking subtle variations in internal tissue conductivity (Mansouri et al., 2021). The four-terminal method largely eliminates this issue: since the voltage-sensing electrodes draw negligible current, the voltage drop at the electrode interface is minimal, and the measured voltages reflect primarily the internal impedance distribution rather than contact artifacts (Saulnier et al., 2001). This makes dynamic physiological changes (such as ventilation-induced impedance variation in the lungs) much more clearly observable. As a result, tetrapolar measurement has become the universal standard in both clinical and experimental EIT hardware.

2. Hardware in context

EIT relies heavily on its hardware architecture, as the accuracy of reconstructed conductivity distributions is limited by the precision and stability of the measurement electronics. Although the EIT principle is conceptually simple (inject alternating current and measure boundary voltages) the inverse problem is highly ill-posed, meaning even small hardware errors propagate directly into image artifacts or mislocalization of structures (Saulnier et al., 2001). Therefore, modern EIT systems require carefully designed subsystems for controlled excitation, high-speed electrode switching, and low-noise, frequency-selective voltage detection.

2.1 Current Excitation Source

At the foundation of every EIT system is a stable AC excitation source capable of delivering a consistent, sinusoidal stimulus to the electrode pair. Because biological tissues exhibit frequency-dependent and spatially varying impedance, the excitation must maintain amplitude stability even as load conditions shift during respiration or pathology. Research-grade and open-source EIT systems commonly employ voltage-to-current conversion circuits (e.g., Howland-based topologies) to approximate constant-current behavior, improving linearity and reducing sensitivity to electrode impedance (Brazey et al., 2022).

In typical systems, excitation amplitudes fall between 0.1–2 mA for phantom experiments, and clinical devices are constrained by IEC 60601, which limits patient-applied AC currents to ≤100 μA (Creegan et al., 2024; Brazey et al., 2022). Frequencies between 1–100 kHz are commonly used depending on whether the goal is static imaging, differential imaging, or multi-frequency characterization. Because the injected current is the reference for all subsequent measurements, amplitude instability or drift directly corrupts the recorded voltage data.

2.2 Electrode Switching Network (Multiplexer Matrix)

To obtain sufficient boundary measurements for image reconstruction, EIT systems must cycle through many different injection and sensing configurations. This is achieved using analog multiplexers, which electronically route the excitation signal to selected electrode pairs while also routing the resulting electrode voltages to the measurement frontend (See Figure 1).

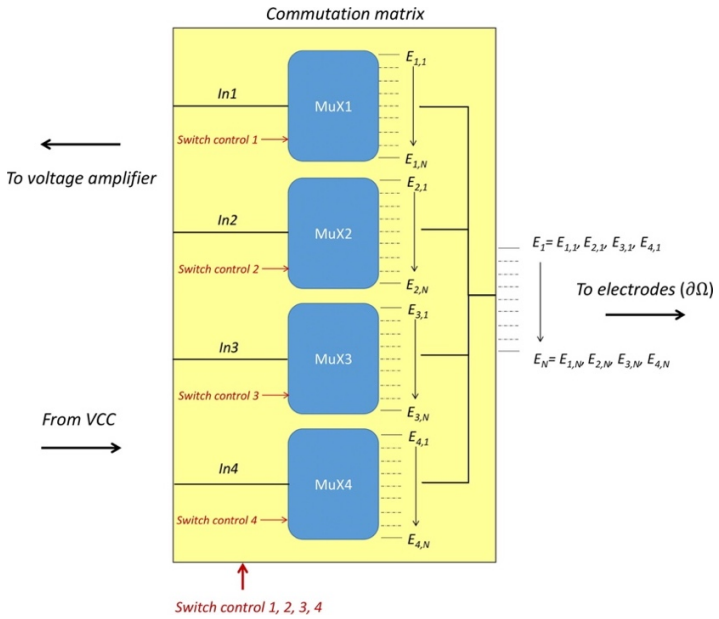

Figure 1[1]: *Figure representing an analog multiplexer (N:4). The purpose of this figure is to illustrate the flow of hardware. Arrows on the left correspond to any current being sent and voltage differences that are going to be read. The commutation matrix uses 4 N:1 multiplexers to route signals (4 = 2 for current injection + 2 for voltage readings). The arrow on the right corresponds to the system we want to observe that has N amount of electrodes.*

Multiplexing dramatically reduces hardware footprint compared to a dedicated channel per electrode and enables rapid sequencing of current patterns used in both adjacent-drive and opposite-drive schemes (Creegan et al., 2024). Because multiplexer switching introduces transient artifacts and parasitic resistances, high-quality switching networks and timing control are necessary to maintain measurement consistency, especially given that EIT voltages typically lie in the tens of microvolts to millivolts range (Saulnier et al., 2001).

[1] Benoit Brazey, et al. "An Open-Source and Easily Replicable Hardware for Electrical Impedance Tomography." HardwareX, vol. 11, 1 Apr. 2022, pp. e00278–e00278, https://doi.org/10.1016/j.ohx.2022.e00278.

2.3 Lock-In Amplifier

A key advancement in modern EIT instrumentation is the integration of a lock-in amplifier, which enables extremely high sensitivity by isolating only the voltage component at the known excitation frequency. Instead of measuring raw electrode voltages (which are typically buried under motion artifacts, environmental interference, and multiplexer-induced noise) a lock-in amplifier performs phase-sensitive detection: it multiplies the measured signal by a reference sinusoid (the same frequency used for injection) and applies narrowband filtering. This produces a clean DC signal proportional to impedance, even when the original AC voltage is at or below the noise floor (Brazey et al., 2022). Because EIT voltages can be orders of magnitude smaller than surrounding noise sources, synchronous demodulation is essential for reliable image formation; without it, boundary voltage data would be too unstable to reconstruct meaningful conductivity maps (Saulnier et al., 2001).

Other than the electrical components used to create a physical EIT system, we would also need a body to attach electrodes that represent the internal conductivity distribution of the physiological system we want to observe. Since EIT can be used to represent many systems, I will not get into the hardware required to recreate a generic system here; however, later in the paper, I will include our approach to building a physical phantom representing the thoracic space for tuberculosis diagnostics purposes.

3. Reconstruction and Digital Modeling

EIDORS (Electrical Impedance and Diffuse Optical Reconstruction Software) is an open-source MATLAB toolbox used extensively in EIT research for both forward and inverse modeling. Its primary function is to provide a computational environment for predicting and interpreting boundary voltage measurements generated by selected current injection patterns. EIDORS

implements the finite-element method (FEM) to approximate solutions to the governing conductivity equation and supports electrode modeling, mesh generation, and regularized image reconstruction. By integrating these components, EIDORS enables reproducible simulations of EIT systems in controlled digital environments. The software separates the modeling pipeline into two stages: the forward model and the inverse model. The forward model defines the domain geometry, electrode configuration, mesh resolution, and current drive patterns, and computes the resulting surface voltages for a specified conductivity distribution (See Figure 1 for conductivity-based constructed model). The inverse model applies regularization-based reconstruction techniques to estimate conductivity changes from measured or simulated voltages and uses that data to create a conductivity-based reconstructed image (See Figure 2). This design permits examination of how geometric assumptions, conductivity changes, and electrode configurations influence image quality.

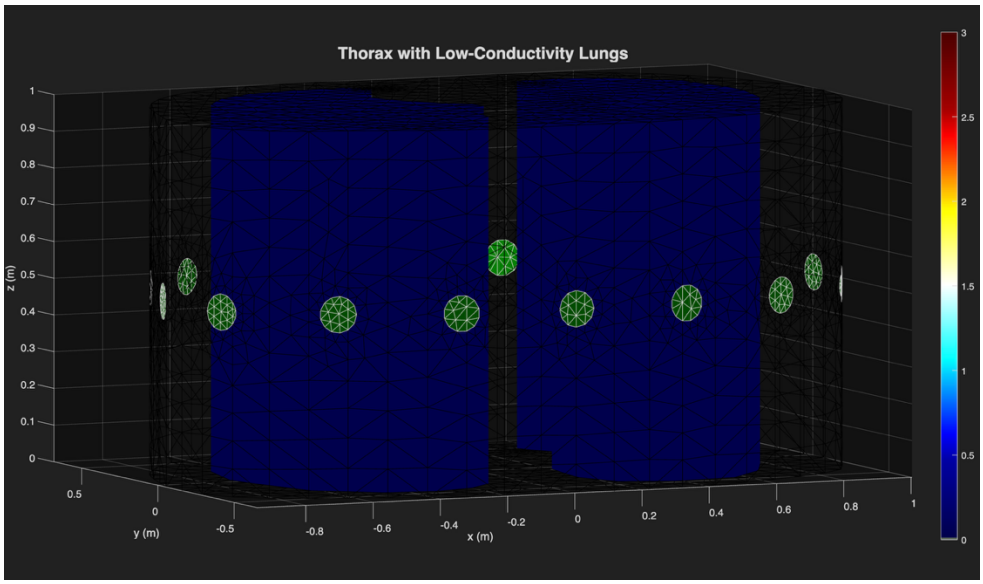

Figure 2: *Pre-meshed human thorax model with a 16-electrode band. The bar on the right represents conductivity (S/m). The thoracic conductivity (background conductivity) is set to 0.25 S/m (and used as a reference, hence the transparent background), and lungs are set to 0.05 S/m.*

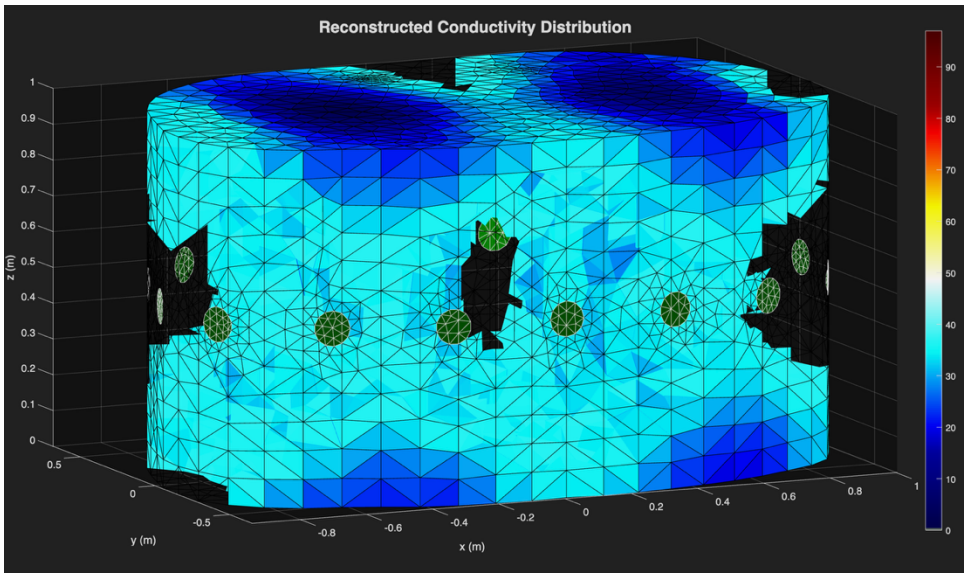

Figure 3: *Reconstructed image from simulated voltage data and solving the inverse problem. The bar on the right represents the conductivity difference, specifically:* $\Delta\sigma = \sigma_{inhomogeneous} - \sigma_{homogeneous}$
Inhomogeneous refers to the model when the low-conductivity regions (lungs) are added.

EIDORS is widely adopted because it provides transparency in modeling decisions, supports complex anatomical geometries, and offers a standardized platform for evaluating reconstruction algorithms. Its use is particularly suited to benchtop EIT development, where digital phantoms serve to predict measurement behavior before physical experimentation. For applications involving thoracic imaging, EIDORS allows exploration of sensitivity distributions, expected voltage changes associated with ventilation, or non-conductive inclusions.

4. Applications of EIT

EIT has emerged as a versatile physiological imaging method because many biological processes produce measurable variations in electrical conductivity. Among all potential uses, thoracic and pulmonary monitoring remains the most clinically validated and widely implemented application of EIT. When air content in the lungs changes during inspiration and expiration, the resulting conductivity variations create strong impedance contrasts that can be captured by surface electrodes in real time (Teschner et al., 2010). Clinical EIT devices such as the Dräger PulmoVista

500 and the SenTec LuMon system continuously visualize regional ventilation distribution, enabling bedside assessment of lung recruitment, overdistension, regional compliance, and ventilation asymmetry in critically ill patients (Teschner et al., 2010; SenTec AG, 2020). This capability is particularly useful during PEEP titration, detection of silent spaces, and monitoring responses to ventilatory adjustments. Because EIT is radiation-free and portable, it allows repeated or continuous assessment without interrupting care, a key advantage over CT imaging.

Beyond ventilation monitoring, EIT can also extract perfusion-related information, as changes in pulmonary blood volume modulate conductivity. Clinical validation studies included in the PulmoVista documentation demonstrate that contrast-agent–based EIT can estimate perfusion distribution and help differentiate ventilated from perfused regions under various physiological conditions (Teschner et al., 2010).

Additional thoracic applications include detection of pneumothorax, pleural effusion, and regional collapse, all of which generate characteristic impedance signatures that can be monitored dynamically at the bedside (Mansouri et al., 2021). EIT has also been applied to cardiac monitoring, as ventricular filling and ejection generate measurable impedance changes within the thorax. Early work summarized by Saulnier et al. showed that cardiac-related impedance variations can be reconstructed to infer stroke volume, blood flow dynamics, and gross patterns of perfusion, although spatial resolution remains limited due to the inherently three-dimensional current paths and anatomical complexity (Saulnier et al., 2001).

Emerging multi-plane electrode configurations and improved reconstruction algorithms, as described in recent review work, have increased the feasibility of extracting cardiac signals from thoracic EIT waveforms (Mansouri et al., 2021). While thoracic applications dominate current clinical use, EIT is also capable of monitoring cerebral, gastric, and musculoskeletal processes, as

noted in foundational reviews. Brain-related impedance changes arise from shifts in blood volume and fluid content during physiological events, and early studies have explored the feasibility of tracking slow hemodynamic changes or pathological shifts with non-invasive surface electrodes (Saulnier et al., 2001).

Although not yet routine in clinical practice, these exploratory studies demonstrate that EIT can detect small conductivity fluctuations associated with physiological or metabolic activity. Across all use cases, EIT's strengths (portability, radiation-free operation, high temporal resolution, and sensitivity to functional physiological changes) position it as a valuable complement to established imaging modalities. As modern hardware improves signal quality through low-noise multiplexing, lock-in detection, and refined electrode systems (Creegan et al., 2024; Brazey et al., 2022), clinical adoption continues to accelerate, particularly in intensive care and respiratory medicine.

5. Ongoing Work

Now, onto the work conducted by my team under the guidance of Professor Grayson at Northwestern University. Our project adapts several established EIT engineering principles but applies them with a fundamentally different priority. Rather than treating EIT primarily as an imaging modality, our goal is to develop a diagnostic screening tool for upper-lung tuberculosis, specifically by detecting the presence and approximate location of a granuloma inside the thoracic cavity. Because lung tissue is characterized by extremely low conductivity due to its high air content, whereas tissue infiltrates or consolidations exhibit markedly higher conductivity, local deviations from the expected impedance distribution provide a measurable signature of pathological change. Our approach prioritizes robust detection and localization, not high-resolution imaging. Although EIT can produce full 3D reconstructions, interpreting these images requires extensive operator training, and the millivolt-scale voltage changes produced by small

inclusions are often visually subtle. From a clinical usability standpoint, a quantitative measurement-based diagnostic pathway is more practical and more reproducible for non-specialist users.

5.1 EIDORS

A central innovation of our project lies in how we use EIDORS. While most research groups rely on EIDORS primarily to generate tomographic images, we instead use it to implement a best-measurement selection algorithm, allowing the system to function as a granuloma detector rather than as a full imaging device. This repositioning of EIDORS, from an imaging toolbox to a diagnostic signal-selection engine, is one of the most unique aspects of our work. Below is the workflow we developed:

1) We construct self-defined 3D finite-element geometries representing a rabbit thorax: a cylindrical outer boundary and two near-cuboid lungs positioned according to anatomical proportions. This geometry mirrors the physical phantom we are building so that simulated measurement patterns translate directly to hardware.

2) To simulate pathology, we remove a small region from the upper right lung to represent a granuloma or infiltrate, assigning it a higher conductivity consistent with soft tissue. This yields two digital phantoms: a baseline thorax with only the lungs (left, Figure 4) and a granuloma phantom with a localized high-conductivity region replacing part of the lung (right, Figure 5).

3) Using these models, we run large-scale voltage simulations by generating all ordered combinations of four electrodes out of sixteen (16P4), representing every distinct arrangement of two electrodes for current injection and two for voltage sensing. Since $^{16}P_4 = 43{,}680$, this produces 43,680 simulated measurements per model, giving us a complete measurement space from which

to analyze how localized conductivity changes alter boundary voltages (See figures 6 and 7 for ΔV measurements from the model with and without the granuloma).

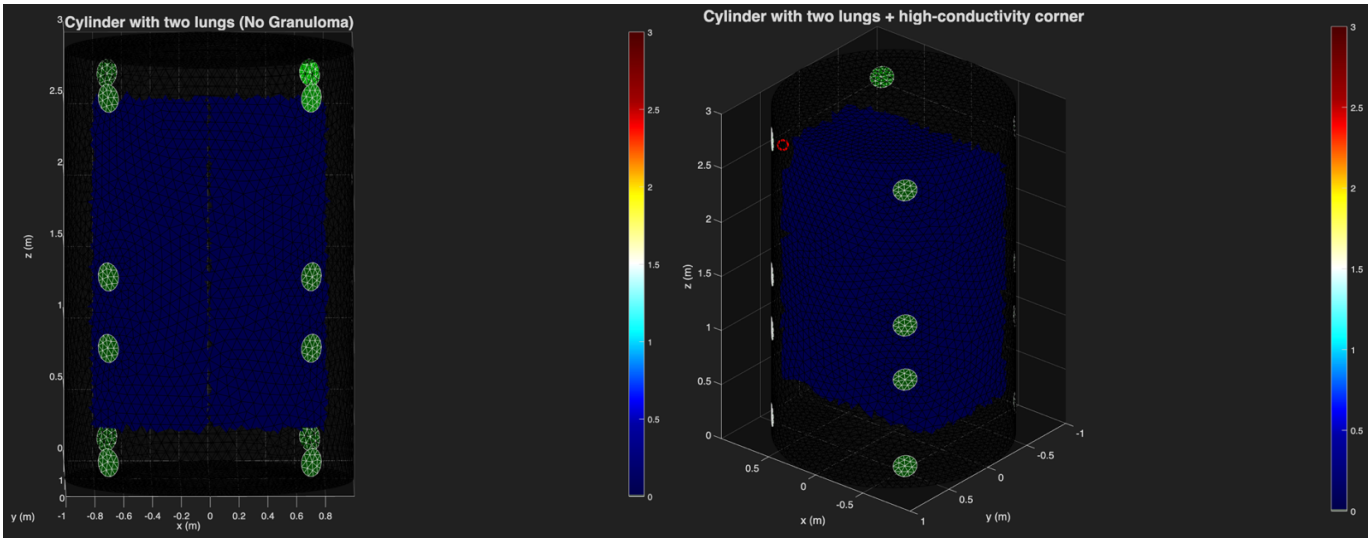

Figures 4 and 5: *Baseline and Granuloma Digital Phantom Models Used for EIDORS Simulation*
Left (Figure 4): *Baseline thoracic model consisting of a cylindrical boundary and two low-conductivity lung volumes.* ***Right (Figure 5):*** *Granuloma model in which a small region of the upper right lung has been removed and assigned a higher tissue-like conductivity (background conductivity) to simulate an insertion. The red dot indicates where the corner of the lung would be if a small piece of the lung was not removed.*

4) For each of the 43,680 measurements, we subtract the baseline voltages from the granuloma-model voltages to obtain a ΔV signature that reflects how strongly that specific measurement responds to the presence of the granuloma. Most electrode pairs show only minimal change, whereas others exhibit larger ΔV magnitudes depending on their spatial sensitivity. We rank all measurements by the absolute magnitude of their ΔV values and retain the top ~200 most sensitive configurations, those most influenced by the granuloma at this assumed position and therefore most informative for distinguishing that location from the baseline (Figure 8).

5) Although our full permutation sweep generates 43,680 simulated ΔV values, only a subset of these correspond to physically valid differential voltage measurements. For a 16-electrode tetrapolar system, the maximum number of admissible measurements under any fixed current-drive pair is

$$D_0 = \frac{C_0(C_0 - 3)}{2}$$

which for C_0 $(contact\ number) = 16$ gives 104 valid differential measurement channels. To determine which of these are most informative for localization, we evaluate ΔV sensitivity not for a single granuloma position but for a small set of hypothesized granuloma locations distributed across the upper lung. For each candidate location, we identify the ~200 most sensitive measurement configurations from the permutation sweep; these lists are then pooled and mapped onto the 104-channel physical measurement space. Because many channels are sensitive to the same positional shifts, we apply Sensitivity Volume (SV) independence analysis to remove redundant channels and retain only those that contribute unique positional information (for example, one measurement distinguishing superior vs. inferior positions, another distinguishing left vs. right, and another distinguishing anterior vs. posterior). SV analysis, therefore yields a small set of maximally independent measurement channels, typically on the order of 3–6, which together provide sufficient directional constraints for localizing the granuloma within the thoracic volume.

6) After selecting this reduced measurement set, we use it to construct a data volume for localization. For each candidate granuloma position, EIDORS computes the full forward measurement vector, and we extract only the selected channels to generate a compact ΔV signature associated with that position. Collectively, these signatures form a discrete mapping from spatial coordinates (x, y, z) to points in the reduced measurement space. In the physical phantom, the lock-in amplifier and multiplexer acquire the same reduced set of measurements. Localization is then performed by comparing the experimentally measured ΔV pattern to the simulated data volume: the granuloma is predicted to lie at the position whose simulated signature most closely matches

the measured one. This approach bypasses full tomographic reconstruction and instead uses a small number of highly informative measurements to perform fast, robust, reconstruction-free diagnostic localization.

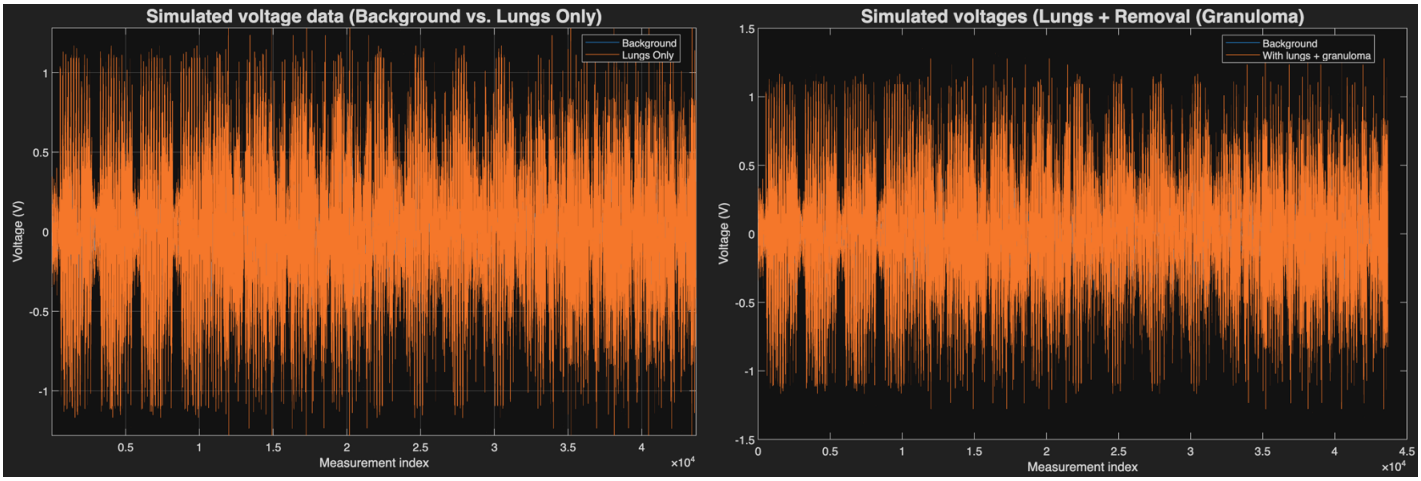

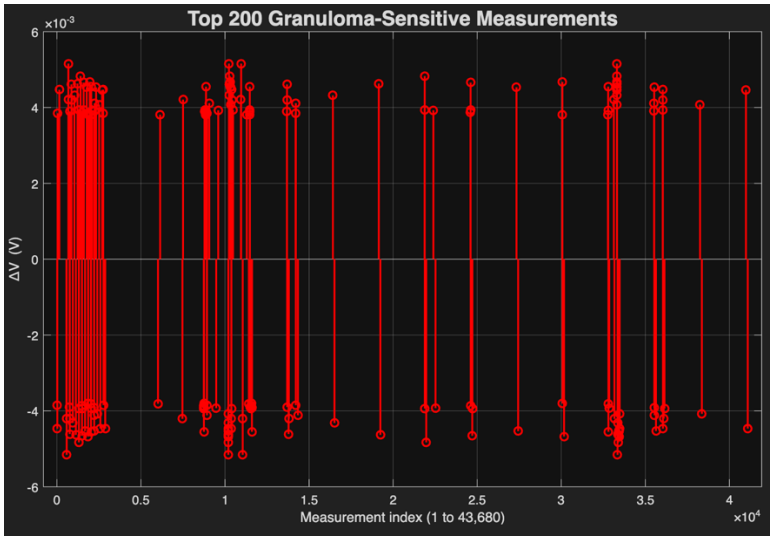

Figures 6, 7, and 8: *Simulated Voltage Measurements and ΔV Ranking for Best-Measurement Selection* ***Left (Figure 6):*** *Simulated voltages for the baseline thoracic model (no granuloma).* ***Right (Figure 7):*** *Simulated voltages for the granuloma model with a high-conductivity corner removed.* ***Bottom (Figure 8):*** *Ranked ΔV values obtained by subtracting Figure 6 from Figure 7, highlighting the ~200 most sensitive measurements used for subsequent selection.*

5.2 Physical Phantom

To validate our EIDORS simulations, we constructed a physical thoracic phantom modeled directly after the digital geometry. The phantom consists of a 1-L saline-filled container

representing conductive thoracic tissue, with two molded polymer-clay lung inserts shaped to approximate rabbit lung dimensions and held in a fixed position using an internal acetyl-rod support structure. Sixteen electrodes are mounted around the outer surface in the same circumferential arrangement used in simulation to ensure measurement consistency between models.

Granuloma formation is simulated by removing a small section from the upper-right lung block, creating a region with saline conductivity. This produces a conductivity asymmetry analogous to TB lesions and allows controlled testing of size-dependent detectability. Because the clay inserts can be removed and re-inserted reproducibly, multiple trials with varying granuloma sizes can be conducted under consistent boundary conditions. Using this phantom, the lock-in amplifier and multiplexer system acquire real voltage data for the SVM-selected measurement sets, enabling direct comparison against simulated ΔV vectors and validating the diagnostic workflow in a controlled experimental environment.

5.3 Hardware Integration

Our hardware setup follows the framework described earlier: a SR830 lock-in amplifier provides a stable sinusoidal current output, which we use directly as the excitation source for the phantom, while the same instrument performs phase-sensitive voltage detection. A custom analog multiplexer routes any of the sixteen electrodes into the drive-positive, drive-negative, sense-positive, or sense-negative roles required by our six optimal measurement configurations.

6. Conclusion

Electrical Impedance Tomography has progressed substantially from its early experimental roots into a clinically meaningful imaging and monitoring modality. Its unique combination of non-

invasiveness, real-time operation, bedside accessibility, and sensitivity to functional physiological changes positions EIT as a valuable complement to established radiological techniques. Continued developments in hardware have greatly improved the stability and fidelity of boundary measurements.

Parallel advances in computational modeling, finite-element solvers, and open-source toolkits such as EIDORS have expanded the feasibility of three-dimensional imaging and enabled rapid prototyping of new algorithms and system architectures.

Despite these strengths, challenges remain. The inverse problem is fundamentally ill-posed, spatial resolution is limited by diffuse current pathways, and small inclusions produce subtle voltage differences that can be difficult to interpret in conventional reconstructions.

By leveraging EIDORS to identify a reduced set of maximally informative electrode configurations and pairing this with a matched physical phantom and lock-in-based measurement system, we demonstrated how EIT can be reframed as a measurement-driven diagnostic tool. Instead of reconstructing full 3D images, our pipeline localizes conductivity anomalies by comparing a small set of experimentally acquired ΔV values to a parametrized data space generated in simulation. This approach trades image complexity for diagnostic clarity and represents a promising pathway for applications where the presence and approximate location of an inclusion are clinically more important than full volumetric imaging.

**All MATLAB scripts developed for the EIDORS simulations described in this report are included in the repository. For those interested in exploring or reproducing these models, the EIDORS toolbox is available for download at https://eidors3d.sourceforge.net/download.shtml*

7. References

- Benoit Brazey, et al. “An Open-Source and Easily Replicable Hardware for Electrical Impedance Tomography.” *HardwareX*, vol. 11, 1 Apr. 2022, pp. e00278–e00278, https://doi.org/10.1016/j.ohx.2022.e00278.
- Creegan, Andrew, et al. “A Wearable Open-Source Electrical Impedance Tomography Device.” *HardwareX*, vol. 18, 1 June 2024, pp. e00521–e00521, https://doi.org/10.1016/j.ohx.2024.e00521.
- Mansouri, Sofiene, et al. “Electrical Impedance Tomography – Recent Applications and Developments.” *Journal of Electrical Bioimpedance*, vol. 12, no. 1, 1 Jan. 2021, pp. 50–62, https://doi.org/10.2478/joeb-2021-0007.
- Onsager, Claire C, et al. “Sensitivity Volume as Figure-of-Merit for Maximizing Data Importance in Electrical Impedance Tomography.” *Physiological Measurement*, vol. 45, no. 4, 1 Apr. 2024, p. 045004, https://doi.org/10.1088/1361-6579/ad3458.
- Saulnier, G.J., et al. “Electrical Impedance Tomography.” *IEEE Signal Processing Magazine*, vol. 18, no. 6, 2001, pp. 31–43, https://doi.org/10.1109/79.962276.
- SenTec AG. LuMon Electrical Impedance Tomography System: Technical Overview, 2020.
- Teschner, Eckhard, et al. PulmoVista 500 Technical Documentation. Dräger Medical, 2010.